Since January 2020 Elsevier has created a COVID-19 resource centre with free information in English and Mandarin on the novel coronavirus COVID-19. The COVID-19 resource centre is hosted on Elsevier Connect, the company's public news and information website.

Phytomedicine 91 (2021) 153704

Contents lists available at ScienceDirect

Phytomedicine

journal homepage: www.elsevier.com/locate/phymed

Original Article

Effect of dihydromyricetin on SARS-CoV-2 viral replication and pulmonary inflammation and fibrosis

Ting Xiao [a,b,1], Yuli Wei [a,b,1], Mengqi Cui [a,b,1], Xiaohe Li [a,b,1], Hao Ruan [a,1], Liang Zhang [c], Jiali Bao [a,b], Shanfa Ren [a,b], Dandi Gao [a,b], Ming Wang [a], Ronghao Sun [a,b], Mingjiang Li [c], Jianping Lin [a], Dongmei Li [a,*], Cheng Yang [a,b,*], Honggang Zhou [a,b,*]

[a] State Key Laboratory of Medicinal Chemical Biology, College of Pharmacy and Tianjin Key Laboratory of Molecular Drug Research, Nankai University, Haihe Education Park, 38 Tongyan Road, Tianjin 300353, People's Republic of China
[b] Tianjin Key Laboratory of Molecular Drug Research, Tianjin International Joint Academy of Biomedicine, Tianjin, China
[c] Department of Thoracic Surgery, Tianjin First Central Hospital, Nankai University, 300192 Tianjin, People's Republic of China

ARTICLE INFO

Keywords:
COVID-19
SARS-CoV-2 M^{pro}
Dihydromyricetin
Pulmonary inflammation
Pulmonary fibrosis

ABSTRACT

Background: COVID-19 (Coronavirus Disease-2019) has spread widely around the world and impacted human health for millions. The lack of effective targeted drugs and vaccines forces scientific world to search for new effective antiviral therapeutic drugs. It has reported that flavonoids have potential inhibitory activity on SARS-CoV-2 M^{pro} and anti-inflammatory properties. Dihydromyricetin, as a flavonol, also has antiviral and anti-inflammatory potential. However, the inhibition of dihydromyricetin on SARS-CoV-2 M^{pro} and the protective effect of dihydromyricetin on pulmonary inflammation and fibrosis have not been proved and explained.

Purpose: The coronavirus main protease (M^{pro}) is essential for SARS-CoV-2 replication and to be recognized as an attractive drug target, we expect to find the inhibitor of M^{pro}. Novel coronavirus infection can cause severe inflammation and even sequelae of pulmonary fibrosis in critically ill patients. We hope to find a drug that can not only inhibit virus replication but also alleviate inflammation and pulmonary fibrosis in patients.

Methods: FRET-based enzymatic assay was used to evaluate the inhibit activity of dihydromyricetin on SARS-CoV-2 M^{pro}. Molecular docking was used to identify the binding pose of dihydromyricetin with SARS-CoV-2 M^{pro}. The protective effects of dihydromyricetin against BLM-induced pulmonary inflammation and fibrosis were investigated in C57BL6 mice. BALF and lung tissue were collected for inflammation cells count, ELISA, masson and HE staining, western blotting and immunohistochemistry to analyze the effects of dihydromyricetin on pulmonary inflammation and fibrosis. MTT, western blotting, reverse transcription-polymerase chain reaction (RT-PCR) and wound healing were used to analyze the effects of dihydromyricetin on lung fibrosis mechanisms in Mlg cells.

Results: In this study, we found that dihydromyricetin is a potent inhibitor targeting the SARS-CoV-2 M^{pro} with a half-maximum inhibitory concentration (IC_{50}) of 1.716 ± 0.419 μM, using molecular docking and the FRET-based enzymatic assay. The binding pose of dihydromyricetin with SARS-CoV-2 M^{pro} was identified using molecular docking method. In the binding pocket of SARS-CoV-2 M^{pro}, the dihydrochromone ring of dihydromyricetin interact with the imidazole side chain of His163 through π-π stacking. The 1-oxygen of dihydromyricetin forms a hydrogen bond with the backbone nitrogen of Glu166. The 3-, 7-, 3'- and 4'-hydroxyl of dihydromyricetin interact with Gln189, Leu141, Arg188 and Thr190 through hydrogen bonds. Moreover, our results showed that dihydromyricetin can significantly alleviate BLM-induced pulmonary inflammation by inhibiting the infiltration of inflammation cells and the secretion of inflammation factors in the early process and also ameliorate pulmonary fibrosis by improving pulmonary function and down-regulate the expression of α-SMA and

Abbreviations: α-SMA, α-smooth muscle actin; BLM, bleomycin; COVID-19, coronavirus disease 2019; Col I, Collagen-I; Cydn, dynamic compliance; DHM, Dihydromyricetin; ECM, extracellular matrix; Fn, fibronectin; FRET, fluorescence resonance energy transfer; FVC, forced vital capacity; IL-1β, interleukin-1β; IL-6, interleukin-6; Mlg, mouse lung fibroblasts; M^{pro}, main protease; Re, expiratory resistance; Ri, inspiratory resistance; SARS-CoV-2, Severe Acute Respiratory Syndrome coronavirus 2; TGF-β, transform growth factor-β; TNF-α, tumor necrosis factor-α.

* Corresponding author.
E-mail addresses: dongmeili@nankai.edu.cn (D. Li), cheng.yang@nankai.edu.cn (C. Yang), honggang.zhou@nankai.edu.cn (H. Zhou).
[1] These authors contributed equally to this work.

https://doi.org/10.1016/j.phymed.2021.153704
Received 21 April 2021; Received in revised form 6 August 2021; Accepted 7 August 2021
Available online 8 August 2021

fibronectin in vivo. Our results also showed that dihydromyricetin inhibits the migration and activation of myofibroblasts and extracellular matrix production via transforming growth factor (TGF)-β1/Smad signaling pathways.

Conclusion: Dihydromyricetin is an effective inhibitor for SARS-CoV-2 M^{pro} and it prevents BLM-induced pulmonary inflammation and fibrosis in mice. Dihydromyricetin will be a potential medicine for the treatment of COVID-19 and its sequelae.

1. Introduction

In December 2019, novel coronavirus disease (COVID-19) was first discovered and reported in Wuhan, China (Wang et al., 2020; Zhu et al., 2020). It was later named SARS-CoV-2 by the International Committee on Taxonomy of Viruses (ICTV) (Coronaviridae Study Group of the International Committee on Taxonomy of, V 2020) aviridae Study Group of the International Committee on Taxonomy of, 2020) and has rapidly spread to 213 countries in the world. By December 18, WHO had reported 68,033,243 confirmed cases and 1,550,995 deaths around the world. Since the WHO declared a global emergency in January 2020, USA Food and Drug Administration (FDA) has issued an emergency use authorization of remdesivir (Aleem and Kothadia, 2020; Lamb, 2020; Moirangthem and Surbala, 2020), favipiravir (Costanzo et al., 2020; Vora and Tiwaskar, 2020), arbidol (Conti et al., 2020a) and other potential drugs (Luo et al., 2020) for treatment of suspected, or laboratory-confirmed, COVID-19 cases. However, the results of several clinical trials show that the clinical effect of these drugs is not significant (Sanders et al., 2020). There is still an urgent need to develop effective drugs for the treatment of COVID-19. Discovery of small molecules as potential SARS-CoV-2 inhibitors continues to be a major research focus within the scientific and pharmaceutical communities.

SARS-CoV-2 genome consists on about 30,000 nucleotides, its replicase gene encodes two overlapping polyproteins, pp1a and pp1ab, which are needed for virus replication (Gupta, 2020). The main protease (M^{pro}) can digest the polypeptide from more than 11 conserved sites to release functional viral proteins for virus replication (Muramatsu et al., 2013; Wu et al., 2015). Therefore, M^{pro} has been considered a therapeutic target for the development of an effective antiviral treatment (Morse et al., 2020).

Natural products have become the source of the active ingredients of many drugs. Flavonoids are the largest class of polyphenols in higher plants, these polyphenols can perform a series of protective functions in the human body, many of them can interfere with the biological activity of nucleic acids or proteins. Many studies have emphasized the wide range of biological activities of flavonoids, including antioxidants, antiviral, anti-inflammatory(Solnier and Fladerer, 2020). A large number of computer simulations and molecular docking studies have shown that many kinds of flavonoids, such as kaempferol, quercetin, naringenin, catechin and epigallocatechin, have potential inhibitory activity on SARS-CoV-2 M^{pro} (Vijayakumar et al., 2020).

Dihydromyricetin is a flavonol isolated from the leaves and stems of *Ampelopsis grossedentata* (Hand.-Mazz.) W. T. Wang (Vitaceae). It has previously showed antibacterial, antiviral, antitussive, anti-inflammatory and antioxidant properties (Wu et al., 2013). Dihydromyricetin has also shown a low inhibitory activity on SARS-CoV 3CLpro (IC_{50} = 364 μM) using an *in vitro* enzymatic assay and molecular docking experiments (Nguyen et al., 2012). In this study, we evaluated the binding force between dihydromyricetin and SARS-CoV-2 M^{pro} by molecular docking, and detected the inhibit activity use the FRET-based enzymatic assay. We also studied the role of dihydromyricetin on anti-inflammation and improving pulmonary fibrosis.

2. Materials and methods

2.1. Drugs and reagents

Dihydromyricetin (96.68%) was purchased in Topscience Co.Ltd (Shanghai, China). The enzyme activity inhibitor screening kit (contains ebselen (> 98%) as positive control) was purchased from Beyotime Biotechnology (Shanghai, China).

2.2. Molecular modeling

The protein structure (PDB ID: 6LU7) (Jin et al., 2020) of SARS-CoV-2 M^{pro} was extracted from the RCSB Protein Data Bank. The structure was prepared using the Protein Preparation Wizard module in Schrödinger 2017 to remove all crystallographic water molecules, correct side chains with missing atoms, add hydrogen atoms and assign protonation states and partial charges with the OPLS_2005 force field. Then, the protein structure was minimized until the root-mean-square deviation (RMSD) of the nonhydrogen atoms reached less than 0.3 Å. Dihydromyricetin was prepared using the LigPrep module of the Schrödinger 2017 molecular modeling package to add hydrogen atoms, convert 2D structures to 3D, generate stereoisomers and determine the ionization state at pH 7.0 ± 2.0 with Epik (Bhachoo and Beuming, 2017). Using the prepared receptor structure, a receptor grid was generated around the original ligand site of the crystal structure. Then, dihydromyricetin was docked to the receptor using the Glide XP protocol.

2.3. Protease activity assay

Enzyme activity detection adopts fluorescence resonance energy transfer method. The protease assays were performed in 96-well black flat-bottomed plates with a final volume of 100 μl. The SARS-CoV-2 M^{pro}, at a final concentration of 0.3 μM was preincubated for 5 min at 37 °C with different concentration dihydromyricetin (0.39, 0.78, 1.56, 3.125, 6.25, 12.5, 25, 50, 100 and 200 μM) and ebselen (0.01, 0.05, 0.1, 0.5, 1, 5 and 10 μM) in the assay buffer (50 mM Tris, 150 mM NaCl, 1 mM EDTA, 1% glycerol, pH 7.3). The FRET substrate (Dabcyl-KTSAVLQSGFRKME-Edans) is added at a final concentration of 20 μM to the enzymatic reaction mixture for 10 min at 37 °C. The blank control well consists 93 μl assay buffer, 5 μl DMSO and 2 μl substrate (Dabcyl-KTSAVLQSGFRKME-Edans). Enzyme activity control well contains 92 μl assay buffer, 1 μl M^{pro}, 5 μl DMSO and 2 μl substrate, sample wells contains 92 μl assay buffer, 1 μl M^{pro}, 5 μl compound and 2 μl substrate. After incubating at 37 °C for 5 min in the dark, the fluorescence signals (excitation/emission, 340 nm/490 nm) of released EDANS were measured using a multiscan spectrum (Thermo Fisher, Shanghai, China). The results were plotted as dose inhibition curves using nonlinear regression with a variable slope to determine the IC_{50} values by GraphPad Prism. Results Inhibition rate (%) = (RFU 100% enzyme activity control-RFU sample) / (RFU 100% enzyme activity control-RFU blank control) × 100%.

2.4. Animals and bleomycin administration

Male C57BL/6 mice (6–8 wk, 20–25 g) had bought from Charles River Laboratories (Beijing, China). All animal care and experimental

procedures complied with guidelines approved by the Institutional Animal Care and Use Committee (IACUC) of Nankai University (Permit No. SYXK 2014-0003). Mice were housed under controlled temperature (22-26 °C), humidity (60 ± 2%) and a 12 h light–dark cycle. Mice had free access to food and water during the whole experiment.

For intratracheal bleomycin (BLM) administration, mice were anesthetized with an intraperitoneal injection of 1% pentobarbital sodium and then intratracheally injected with 2.5 U/kg BLM (Hanhui Pharmaceuticals CO., LTD, Hangzhou, China). For control group the same amount of saline was injected intratracheally by the same method. For fibrosis model, 30 mice were divided into six groups, with 5 mice *per* randomly assigned group: control group, BLM group, BLM + pirfenidone group (200 mg/kg), BLM + dihydromyricetin group low dose (DM LD) (50 mg/kg), BLM + dihydromyricetin group medium dose (DM MD) (100 mg/kg), BLM + dihydromyricetin group high dose (DM HD) (200 mg/kg). Pirfenidone (Meilunbio, Dalian, China) was used as the positive control. The mice in the drug administration group were intragastrically administered with pirfenidone or dihydromyricetin daily from the 7 th day to 14 th day after BLM injury. Control and BLM group were received the same amount of saline. Mice were sacrificed on the 14 th day after BLM administration to evaluate the degree of pulmonary fibrosis. The inflammation model group is the same as the fibrosis model, 30 mice were randomly divided into 6 groups, control group, BLM group, BLM + pirfenidone group (200 mg/kg), BLM + dihydromyricetin group low dose (DM LD) (50 mg/kg), BLM + dihydromyricetin group medium dose (DM MD) (100 mg/kg), BLM + dihydromyricetin group high dose (DM HD) (200 mg/kg). Dihydromyricetin was intragastrically administered daily for 1 week beginning from 1st to 7 th day after BLM injury and mice were sacrificed on the 8 th day after BLM administration for the evaluation of pulmonary inflammation.

2.5. Histological examination

The left lungs were fixed with 4% paraformaldehyde (Solarbio, Beijing, China) for 24 h, and the excess lung tissues were trimmed and embedded in paraffin. The lung sections (5 μm) were prepared and stained with hematoxylin-eosin (H&E) staining (Zsbio, Beijing, China) and Masson's trichrome (Solarbio) for histological examination. The slides with H&E staining were sampled with a random-start systematic sampling scheme using a 6-mm-grid randomly superimposed on the slide to indicate areas to evaluate. Digitized images of the slide were obtained using a photographic Nikon microscope (Nikon, Tokyo, Japan). Images were then opened in Photoshop and the overall area of the lung was obtained by manual outlining. The area of fibrotic lung was then outlined. The pixels of total versus fibrotic tissue were then summed over each lung and a percentage was obtained (Jiang et al., 2004).

2.6. Bronchoalveolar lavage fluid

For bronchoalveolar lavage fluid (BALF) collection, the trachea of mice was cannulated and lavaged three times with 0.8 ml sterile PBS at room temperature, then the BALF samples were centrifuged at 845 g for 10 min. The supernatant was stored at -80 °C for analysis of inflammatory factors, and the cell pellet was resuspended in 1ml of red blood cell lysate. Then, the lysis buffer was centrifuged at room temperature at 845 g for 10 min, discard the supernatant and resuspend the cell pellet in 200 μl PBS. Total cell count was performed by Countstar automatic cell counting instrument (ALIT Life Science, Shanghai, China). Smears of each suspension were stained with H&E staining for differential cell counting. Macrophages, neutrophils, and lymphocytes were counted under optical microscope using standard morphologic criteria.

2.7. ELISA detection

BALF supernatant was prepared for ELISA detection. The concentration of inflammatory factors including IL-1β, IL-6, and TNF-α was detected by ELISA kits following the manufacturer's protocol.

2.8. Hydroxyproline content determination

Hydroxyproline was tested according to the previously described methods (Li et al., 2019). Briefly, the three mice right lungs were separated and placed in 4 ml ampoules, then dried, acid hydrolyzed at 120 °C and adjust the pH to 6.5-8.0. The results were calculated as μg hydroxyproline *per* right lung using hydroxyproline standards (Sigma Aldrich, Shanghai, China). The hydroxyproline analysis was performed using chloramine-T spectrophotometric absorbance.

2.9. Pulmonary function measurement

The pulmonary function of C57BL/6 mice were measured using AniRes2005 lung function system (Bestlab, Beijing, China) according to the manufacturer's instructions. To detect the ventilation-associated pressure change inside the chamber, the Anires2005 system automatically calculates and displays pulmonary function parameters, such as inspiratory resistance (Ri), expiratory resistance (Re), dynamic compliance (Cdyn) and forced vital capacity (FVC).

2.10. Immunohistochemistry

Paraffin-embedded lung tissue sections were deparaffinized with xylene and repaired at high temperature for 2 min. Use the ready-to-use immunohistochemical UltraSensitiveTM SP kit (Maxin, Shenzhen, China) according to the instructions to process the slices, and then use DAB staining solution (Solarbio) for color reaction. After nuclear staining with hematoxylin, the sections were observed under an optical microscope.

2.11. Western blotting

All proteins were extracted from lung tissues as reported previously (Ning et al., 2004). The proteins were separated by polyacrylic gel electrophoresis and transferred to polyvinylidene difluoride (PVDF) membrane (Roche, Basel, Switzerland). After blocking with 5% skim milk for 1 h, the membranes were incubated at 4 °C overnight with monoclonal antibodies against α-SMA, Fibronectin and β-tubulin. Then, the membranes were incubated with HRP-conjugated secondary antibodies (Abcam, Cambridge, UK) for 2 h at room temperature and tested with chemiluminescence reagent (Affinity, Pottstown, PA, USA).

2.12. Cell culture

The mouse lung fibroblasts (Mlg) were kindly provided by Professor Wen Ning (Nankai University, Tianjin, China) and were maintained in DMEM (Solarbio) containing 10% FBS (Gibco, Carlsbad, CA, USA) and 1% penicillin–streptomycin (Gibco). Cells were cultured in a constant temperature incubator with 5% CO_2 at 37 °C.

2.13. Real-time quantitative PCR

Total RNA was extracted from cells using trizol (Thermo Scientific Inc, Waltham, MA, USA) according to the manufacturer's instructions. Transcription was performed using the Reverse SYBR Select Master Mix kit, according to the instructions (Tiangen, Beijing, China), followed by fluorescence quantitative real-time PCR (Yeasen, Shanghai, China). α-SMA:forward primer: 5'- GCTGGTGATGATGCTCCCA-3'; reverse primer: 5'- GCTGGTGATGATGCTCCCA-3'; Collagen I: forward primer: 5'- CCAAGAAGACATCCCTGAAGTCA-3'; reverse primer: 5'- TGCACGTCATCGCACACA -3'; Fibronectin: forward primer: 5'- GTGTAGCACAACTTCCAATTACGAA-3'; reverse primer: 5'- GGAATTTCCGCCTCGAGTCT-3'; *GAPDH*: forward primer: 5'- GGGGTCGTTGATGGCAACA-3'; reverse primer: 5'-

AGGTCGGTGTGAACGGATTTG-3'.

2.14. Wound-healing assays

The Mlg cells were inoculated in six-well plates for the wound healing assay, and were scraped to form a wound by using 200 μl sterile pipette tips. After washing with phosphate buffer, add TGF- β 1 (5 ng/ml) or dihydromyricetin (10, 20 and 40 μM) and take images at 0, 6, 12 and 24 h to observe cell migration by using a light microscope (Nikon).

2.15. Statistical analysis

GraphPad Prism 7.0 was used for statistical analysis. Differences between experimental and control group were assessed by Student's *t* test. Significant differences among multiple groups were detected by one-way ANOVA. $P < 0.05$ was considered as statistically significant.

3. Results

3.1. The structural basis and enzyme inhibitory activity of dihydromyricetin on SARS-CoV-2 M^{pro}

We docked the dihydrimyricetin to SARS-CoV-2 M^{pro}. The 2D structures of the dihydromyricetin and the corresponding Glide XP docking scores are shown in Fig. 1A. We also identified the structural basis of dihydromyricetin and M^{pro}. The docked binding pose and the interaction details of dihydromyricetin with SARS-CoV-2 M^{pro} are presented in Fig. 1B. The dihydrochromone ring of dihydromyricetin forms a π-π interaction with the imidazole side chain of His163. The 1-oxygen of dihydromyricetin forms a hydrogen bond with the backbone nitrogen of Glu166. The 3- and 7-hydroxyl of dihydromyricetin forms hydrogen bonds with the side chain oxygen of Gln189 and the backbone oxygen of Leu141. The 3'- and 4'-hydroxyl of dihydromyricetin form hydrogen bonds with the backbone oxygen of Arg188 and the backbone oxygen of Thr190.

The results of molecular docking are encouraging, so we then further confirmed the inhibitory activity of dihydromyricetin in a dose gradient by FRET-based enzyme activity assay. Dihydromyricetin inhibited SARS-CoV-2 M^{pro} with $IC_{50} = 1.716 \pm 0.419$ μM (Fig. 2A). Ebselen, as the positive control drug, inhibited SARS-CoV-2 M^{pro} with $IC_{50} = 1.629 \pm 0.212$ μM (Fig. 2B).

3.2. Dihydromyricetin reduces the inflammatory response in BLM-treated mice

To investigate the anti-inflammatory role of dihydromyricetin on lung injury, a BLM-induced lung injury model was built, dihydromyricetin was administered continually for 7 days, and pirfenidone acted as a positive control (Fig. 3A). The results of H&E staining of lung pathological sections showed that dihydromyricetin improved the inflammatory cell infiltration and restored alveolar structure in BLM-injured lung tissues (Fig. 3B). The total population and differential subsets inflammatory cell numbers were significantly up-regulated in BALF of BLM-treated mice, and dihydromyricetin administration significantly down-regulated the number of inflammatory cells (Fig. 3C-F). In addition, we detected the expression levels of inflammatory factors including

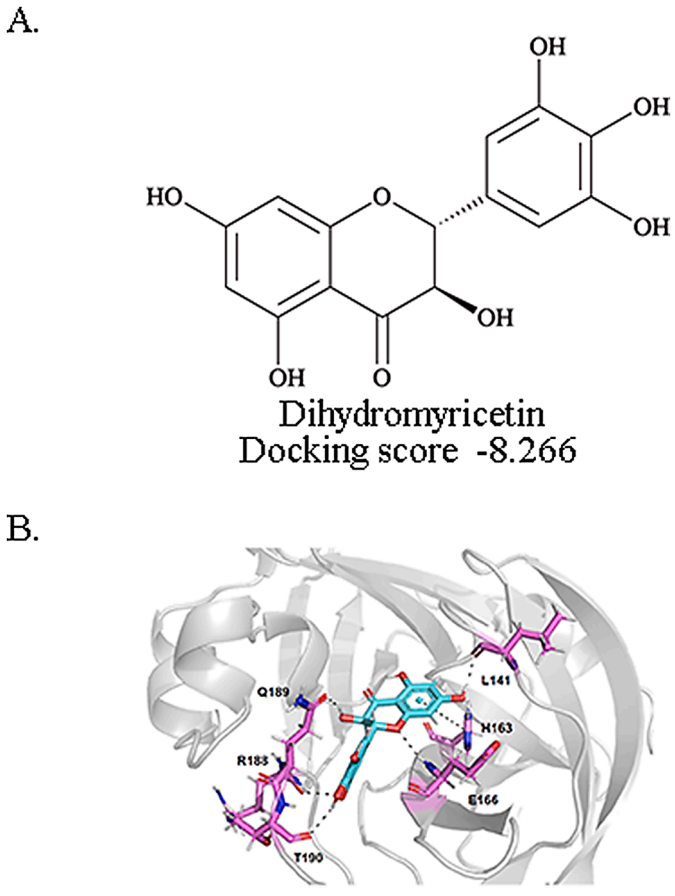

Fig. 1. Docked conformations of dihydromyricetin in SARS-CoV-2 M^{pro} proteases and the inhibitory activity of dihydromyricetin in vitro. A. The structure and docking score of dihydromyricetin. B. Dihydromyricetin docking to the SARS-CoV-2 M^{pro} protein X-ray structure (Protein Data Bank accession No.6LU7).

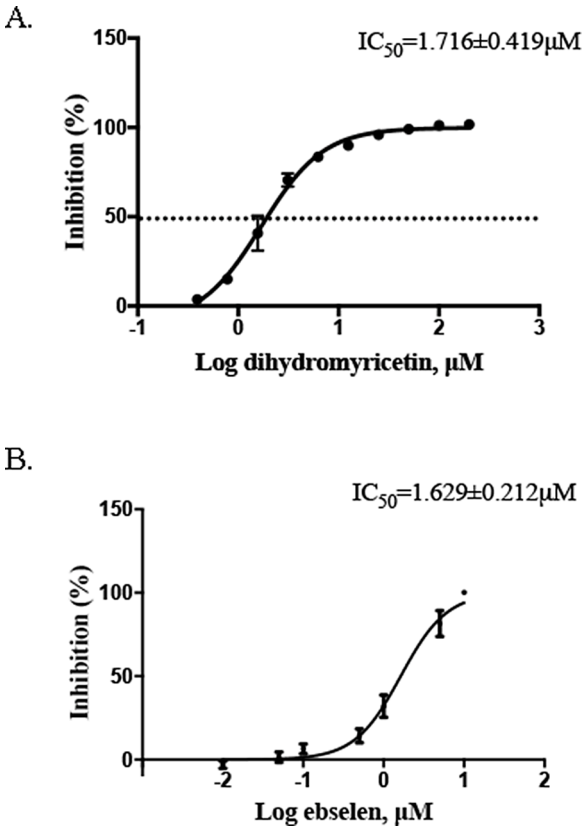

Fig. 2. Inhibition of SARS-CoV-2 M^{pro} activity by dihydromyricetin and ebselen. Protease activities of SARS-CoV-2 M^{pro} in the presence of inhibitors were measured by FRET-based enzymatic activity assay. IC_{50} of (A) dihydromyricetin and (B) ebselen. Error bars: mean ± S.D. of three independent replicates.

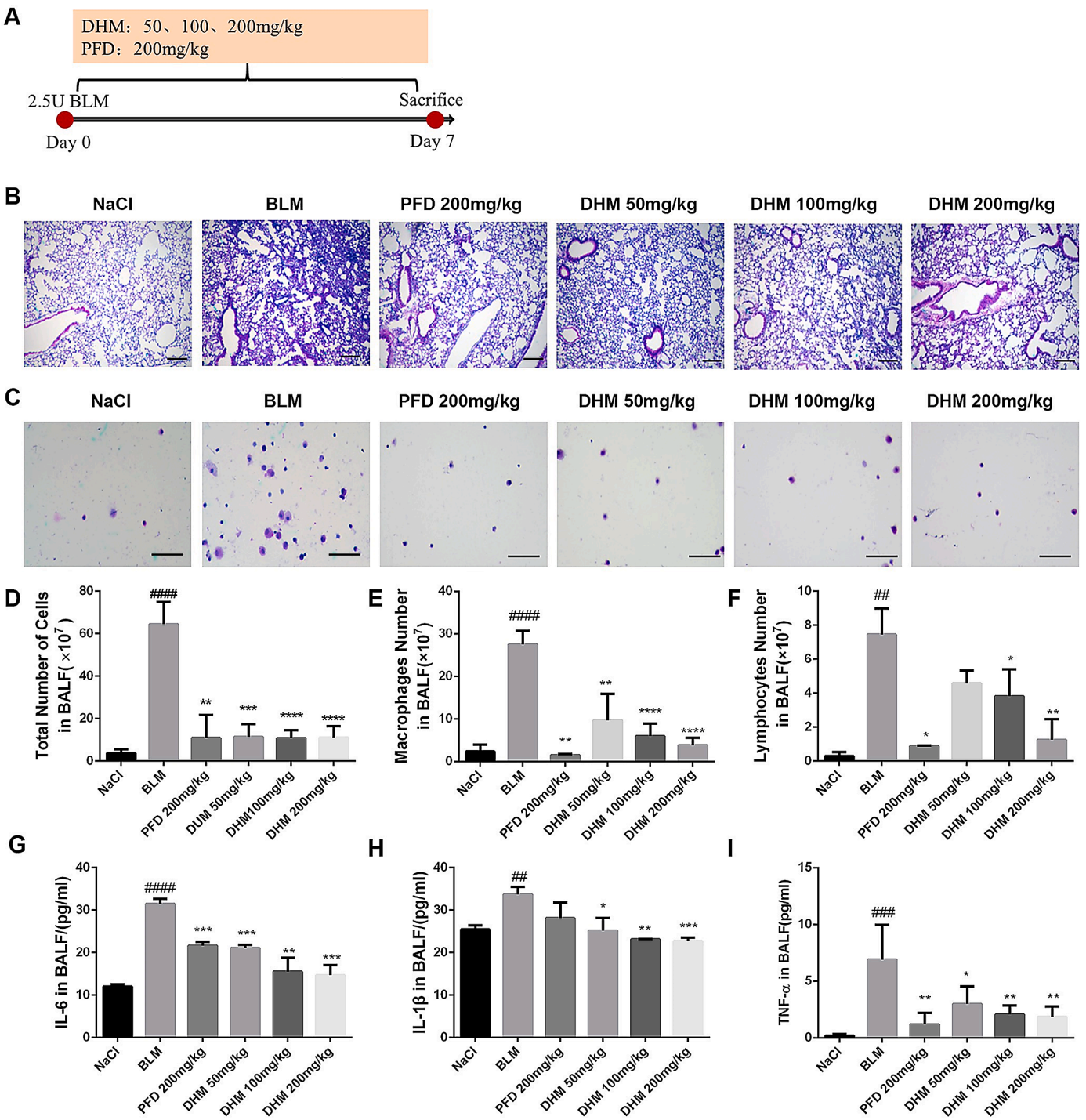

Fig. 3. Effect of dihydromyricetin on reduce the inflammatory response in BLM-treated mice. (A) Dosing regimen in BLM-induced inflammatory model. (B-C) H&E staining of left lung tissues (B, Scale: 50 μm) and inflammatory cells in BALF (C, Scale: 20 μm) of each group. (D) Total number of cells from BALF in each group. (E) Counts of macrophages in BALF. (F) Counts of lymphocytes in BALF. (G-I) The expression of inflammatory factors including IL-6, IL-1β and TNF-α in BALF were detected by ELISA. Data are shown as mean ± SD. # represent the difference between NaCl and BLM-treated group, ## $p < 0.01$, ### $p < 0.001$, #### $p < 0.0001$. * represent the difference between BLM-treated and treatment group, * $p < 0.05$, ** $p < 0.01$, *** $p < 0.001$, **** $p < 0.0001$.

IL-6, IL-1β, and TNF-a in BALF, and the results showed that dihydromyricetin significantly inhibited the expression levels of inflammatory factors (Fig. 3G-I). These data indicated that dihydromyricetin could reduce the pulmonary inflammatory response in BLM-treated mice.

3.3. Dihydromyricetin alleviates BLM-induced pulmonary fibrosis in mice

To further detect the therapeutic role of dihydromyricetin on pulmonary fibrosis, the BLM-induced animal model of pulmonary fibrosis was built, dihydromyricetin was administered *per* day from day 7 to day 14 after BLM injury, and pirfenidone acted as a positive control (Fig. 4A). Compared with the model group, the collagen content and fibrosis area in the lungs of the DM HD group were reduced about 2-fold

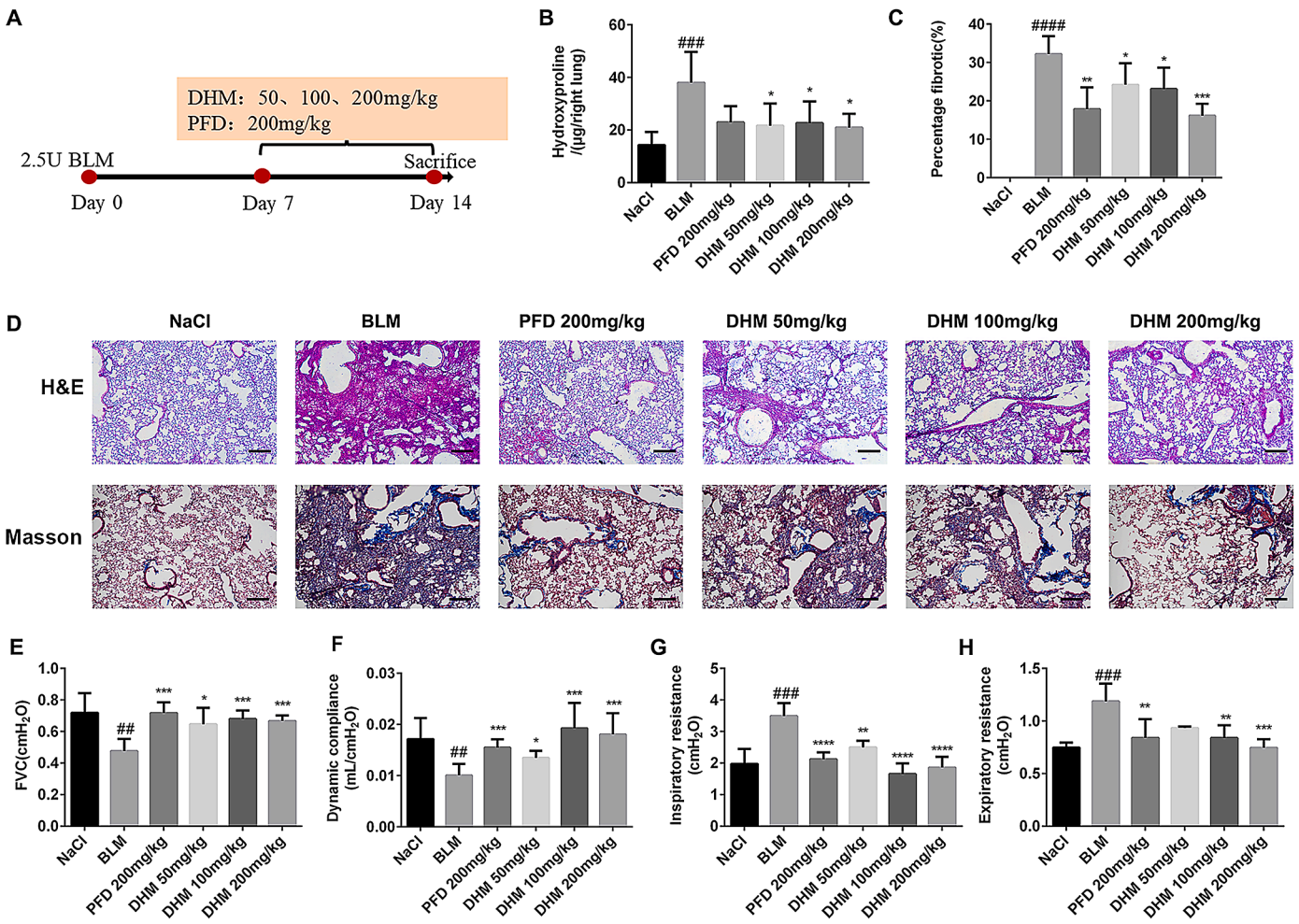

Fig. 4. Effect of dihydromyricetin on pulmonary fibrosis and improves pulmonary function in BLM-treated mice. (A) Dosing regimen in BLM-induced fibrosis model. (B) Hydroxyproline content of lung tissues in each group. (C) Statistics of lung fibrosis area in each group. (D) Photomicrographs of H&E staining and Masson staining of lung tissues (Scale: 50 μm). (E-H) Lung function parameters, include forced vital capacity (FVC), dynamic compliance (Cydn), inspiratory resistance (Ri) and expiratory resistance (Re). Data are shown as mean ± SD. # represent the difference between NaCl and BLM-treated group, ## $p < 0.01$, ### $p < 0.001$, #### $p < 0.0001$. * represent the difference between BLM-treated and treatment group, * $p < 0.05$, ** $p < 0.01$, *** $p < 0.001$, **** $p < 0.0001$.

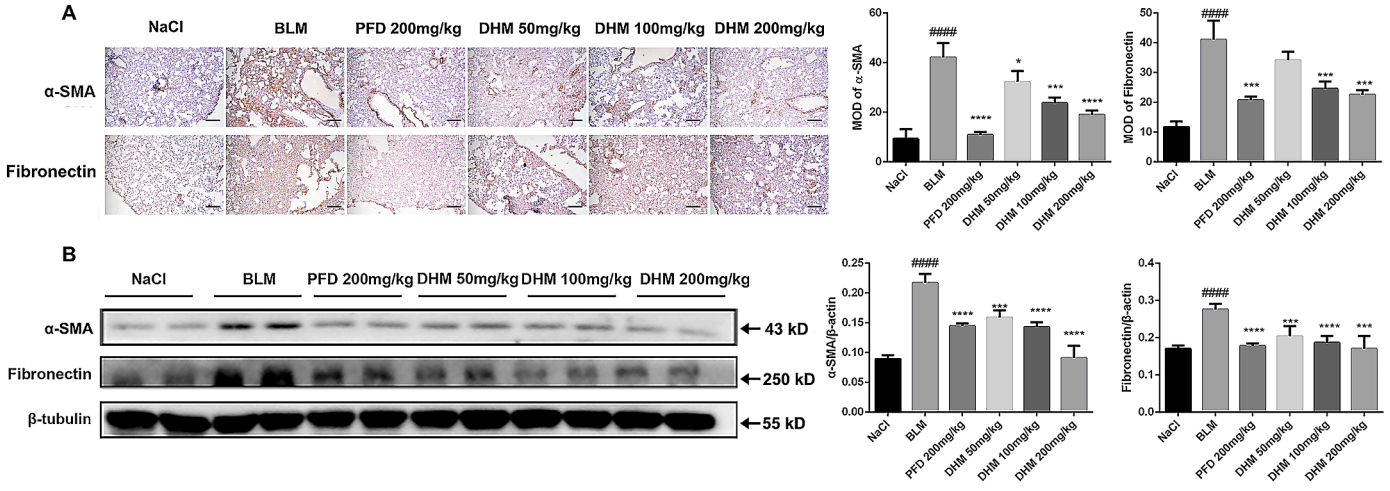

Fig. 5. Effect of dihydromyricetin on BLM-induced myofibroblast differentiation and ECM deposition *in vivo*. (A) Immunohistochemical staining of α-SMA and Fibronectin in the lung tissues (Scale: 50 μm). (B) Western blot analysis of the protein levels of α-SMA and Fibronectin in lung tissues. β-tubulin was used as the internal reference. Data are shown as mean ± SD. # represent the difference between NaCl and BLM-treated group, ## $p < 0.01$, ### $p < 0.001$, #### $p < 0.0001$. * represent the difference between BLM-treated and treatment group, * $p < 0.05$, ** $p < 0.01$, *** $p < 0.001$, **** $p < 0.0001$.

(Fig. 4B-C). The H&E and Masson staining of lung tissue pathological sections also showed that dihydromyricetin could ameliorate alveolar–capillary structure damage and collagen deposition in BLM-injured lung tissues (Fig. 4D). We further measured the changes in pulmonary function between different groups and the results showed that the pulmonary function in dihydromyricetin-treated mice was significantly improved. The forced vital capacity (FVC) and dynamic compliance (Cdyn) of dihydromyricetin-treated mice were increased compared with model group, the FVC of the model group was 0.4760 ± 0.02708 cmH_2O and the FVC of DM HD group was increased to 0.6668 ± 0.01538 cmH_2O ($p = 0.0003$), the Cdyn of the model group was 0.01006 ± 0.0007942 cmH_2O and the Cdyn of DM HD group was increased to 0.01806 ± 0.001859 cmH_2O ($p = 0.0008$). Inspiratory resistance (Ri) and expiratory resistance (Re) were decreased compared with model group, the Ri of the model group was 3.490 ± 0.1556 cmH_2O and the Ri of DM HD group was decreased to 1.861 ± 0.1501 cmH_2O ($p < 0.0001$), the Re of the model group was 1.187 ± 0.06389 cmH_2O and the Re of DM HD group was increased to 0.7452 ± 0.03361 cmH_2O ($p = 0.0001$) (Fig. 4E-H). In order to further verify the anti-fibrosis effect of dihydromyricetin, we performed immunohistochemistry and Western Blot assays to detect the expression levels of fibrosis makers α-SMA and Fibronectin in lung tissues. The results indicated that dihydromyricetin treatment (DM LD, DM MD and DM HD group) significantly decreased the expression of the fibrosis markers in the lung tissues of BLM-injur ed mice (Fig. 5). These results showed that dihydromyricetin could alleviate BLM-induced pulmonary fibrosis.

3.4. Dihydromyricetin suppresses TGF-β1-induced migration of lung fibroblasts

Mouse lung fibroblast (Mlg) cells were exposed to TGF- β 1 (5 ng/ml) or a series dihydromyricetin concentration (0–160 μM) in serum-free medium for 24 h to detect cytotoxicity. The results indicated that dihydromyricetin has no significant cytotoxicity to Mlg cells at 0-160 μM (Fig. 6A). The migration of lung fibroblasts is an important feature of pulmonary fibrosis disease. Our study showed that dihydromyricetin inhibited TGF-β1-induced lung fibroblast migration in Mlg cells (Fig. 6B).

3.5. Dihydromyricetin inhibits lung fibroblast activation and extracellular matrix (ECM) accumulation by down-regulating the TGF- β1/Smad pathway in vitro

TGF-β1/Smad signal plays an essential role in pulmonary fibrotic progression in regulating fibroblast overaction. To further explore the anti-fibrosis effect of dihydromyricetin, we performed Western Blot and quantitative real-time PCR to detect the protein and mRNA expression levels of fibroblasts activation-related maker a-SMA and extracellular matrix (ECM) deposition maker Fibronectin, Collagen I in Mlg cells. Mlg cells were exposed to TGF-β1 (5 ng/ml) and/or dihydromyricetin (10, 20, 40 μM) for 24 h, and the western blot and qRT-PCR results indicated that dihydromyricetin significantly decreased the expression of the fibrosis markers at the concentration of 20 and 40 μM (Fig. 7A-B). Further study showed that dihydromyricetin could reduce the phosphorylation level of p-Smad2 and p-Smad3 at the concentration of 10, 20 and 40 μM (Fig. 7C). In summary, dihydromyricetin could inhibit TGF-β1-induced myofibroblast activation and ECM accumulation.

4. Discussion

With the spread globally of COVID-19, scientists and researchers all over the world are racing to discover potent vaccines and antiviral drugs. Many hopeful drugs, such as remdesivir, lopinavir and ritonavir, recently failed in a clinical trial for COVID-19 (Sanders et al., 2020). So, it is still an urgent need to develop effective antiviral drugs against SARS-CoV-2. SARS-CoV-2 M^{pro} plays a crucial role in the production of viral proteins and controlling the activity of the replicase complex. It is characterized to be an essential and highly potent target for the inhibition of the novel coronavirus (Wu et al., 2020). Many of researches reported that natural products, mainly flavonoids compounds, had good capability to suppress SARS-CoV-2 M^{pro} based on the computer analysis of protein-ligand docking (Abian et al., 2020; Das et al., 2020; Ghosh et al., 2020; Ibrahim et al., 2020). Several studies have reported that rutin, a flavonol glycoside, has high efficacy as a potent inhibitor to treat COVID-19 infection and noncovalent interact with the heteroatoms of amino acids of the M^{pro}'s active sit (Ibrahim et al., 2021). Batool *et al* identified TF-9, a thioflavonol, as a highly promising inhibitor of SARS-CoV-2 M^{pro} with predicted binding energy of -8.7 kcal/mol from 101 synthetic flavonols (Batool et al., 2020). Quercetin was identified as reasonably potent inhibitor of SARS-CoV-2 3CLpro with Ki~7 μM from a small chemical library (Abian et al., 2020). However, there is a lack of clear evidence to prove its effectiveness in *vivo* and *vitro*. In this study, the intermolecular force between dihydromyricetin and SARS-CoV-2 M^{pro} was evaluated by molecular docking. The molecular docking result of dihydromyricetin and M^{pro} showed that dihydromyricetin can bind to M^{pro} at Leu141, Glu166, Gln189 and Thr190 by form hydrogen bonds and at His163 by π-π stacking. Dihydromyricetin occupies the position of the active center of SARS-CoV-2 M^{pro}. Besides, dihydromyricetin exhibits the encouraging inhibit activity of SARS-CoV-2 M^{pro} with IC_{50} of 1.716 ± 0.419 μM.

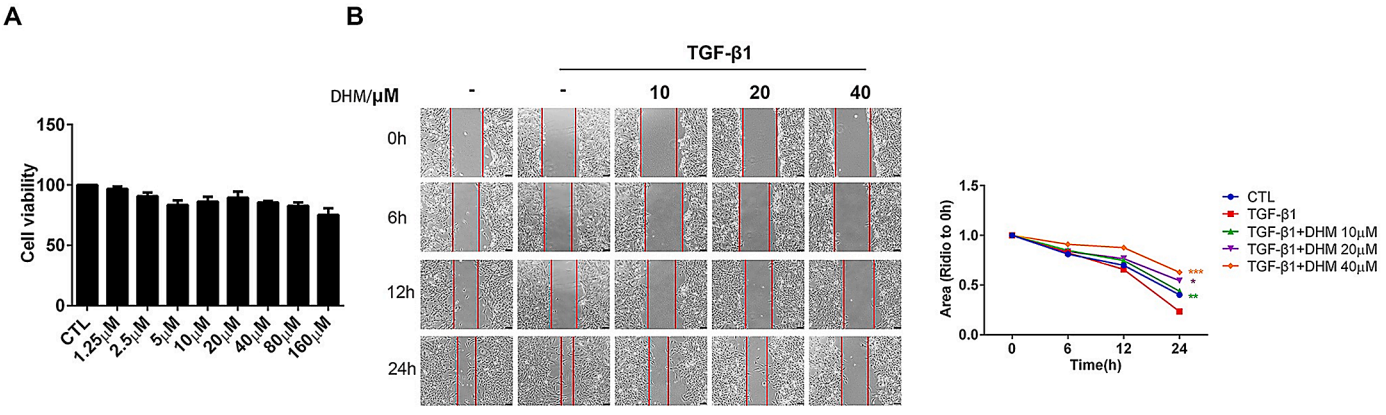

Fig. 6. Effect of dihydromyricetin on TGF-β1-induced migration of pulmonary fibroblasts. (A) Mlg cells were exposed to TGF- β1 (5 ng/ml) or a series dihydromyricetin concentration (0–160 μM) in serum-free medium for 24 h. (B) Mlg cells were treated with TGF-β1 and/or dihydromyricetin (10 μM, 20 μM, 40 μM) for 0, 6, 12, or 24 h. Area analyses are shown beside. Scale bars: 100 μm. Data are shown as mean ± SD. * represent the difference between TGF-β1 treatment and dihydromyricetin-treated group, * $p < 0.05$, ** $p < 0.01$, *** $p < 0.001$, **** $p < 0.0001$.

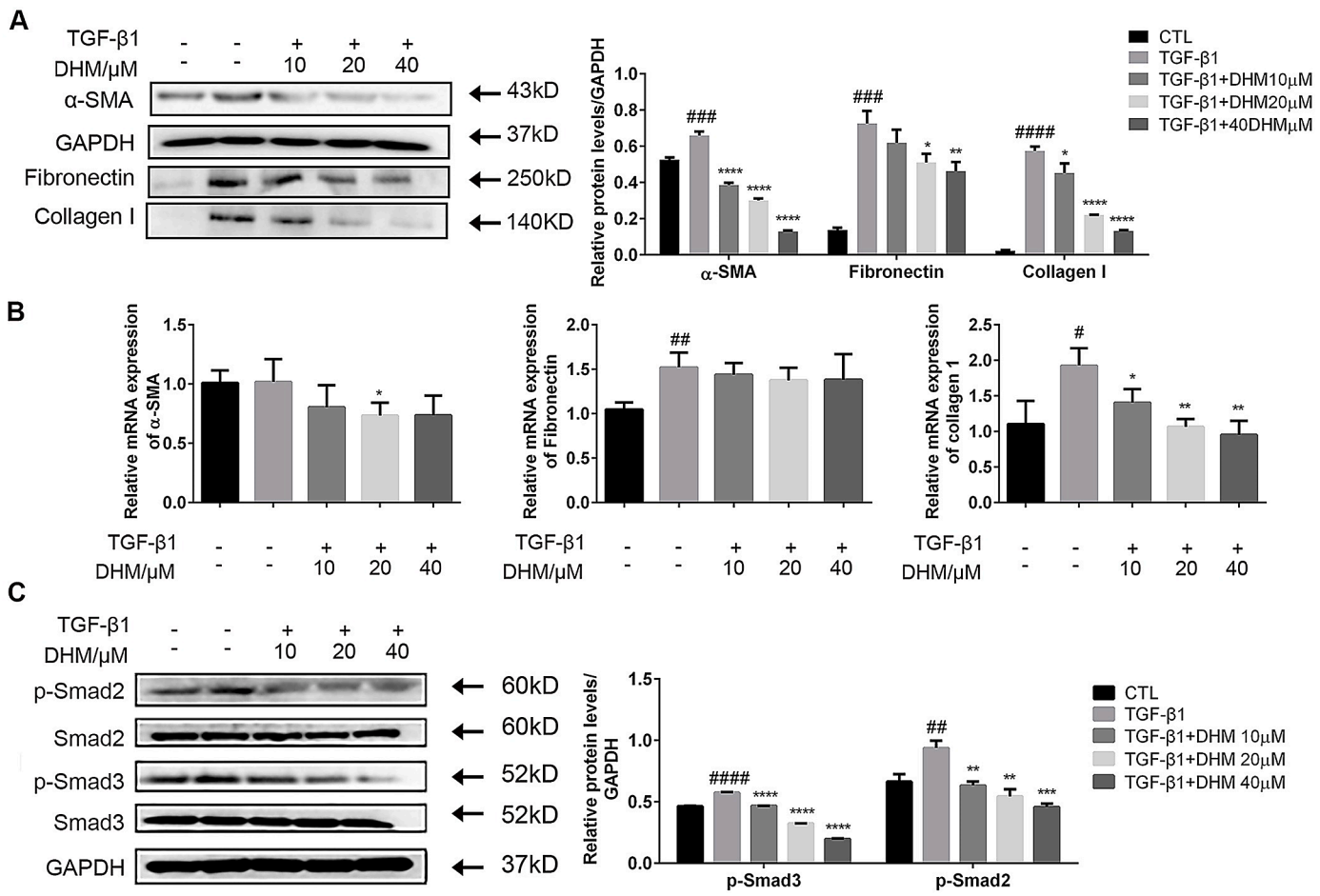

Fig. 7. Effect of dihydromyricetin on fibroblast activation and extracellular matrix (ECM) accumulation by down-regulating the TGF- β 1/Smad pathway *in vitro*. (A) Mlg cells were exposed to TGF-β1 (5 ng/ml) and/or dihydromyricetin (10, 20, 40 μM) for 24 h. The expression level of a-SMA, Collagen I and Fibronectin in cells were detected by Western Blot. (B) Mlg cells were exposed to TGF-β1 (5 ng/ml) and/or dihydromyricetin (10, 20, 40 μM) for 24 h, and quantitative real-time PCR was used to detect the mRNA levels of a-SMA, Collagen I and Fibronectin. (C) Mlg cells were exposed to TGF-β1 (5 ng/ml) and/or dihydromyricetin (10, 20, 40 μM) for 30 min. Detect the expression level of p-Smad2, Smad2, p-Smad3, Smad3 and GAPDH. Data are shown as mean ± SD. # represent the difference between control and TGF-β1 treatment group, ## $p < 0.01$, ### $p < 0.001$, #### $p < 0.0001$. * represent the difference between TGF-β1 treatment and dihydromyricetin-treated group, * $p < 0.05$, ** $p < 0.01$, *** $p < 0.001$, **** $p < 0.0001$.

Severe cases of COVID-19 are characterized by a strong inflammatory process that may ultimately lead to organ failure and patient death and the patients survived from COVID-19 are at risk of chronic respiratory complications such as lung fibrosis, pulmonary thromboembolism, and attendant functional impairment (Conti et al., 2020a; Conti et al., 2020b; Ozma et al., 2020). Dihydromyricetin has the effects of cardioprotection, hepatopretection, neuroprotection and dermatoprotection. It was also applied for the treatment of bacterial infection, liver and kidney injury, asthma and inflammation. It has been verified the anti-fibrotic effect of dihydromyricetin on Ang II stimulated cardiac fibroblasts (Zhang et al., 2018). However, the detailed mechanisms still are not very clear. In our previous study, we reported that myricetin could effectively attenuate pulmonary fibrosis of BLM-treated mice (Li et al., 2020). Here, we evaluated the effect of dihydromyricetin in *vivo* on BLM-induced pulmonary inflammatory and fibrosis, and the results indicated that dihydromyricetin also could effective improve pulmonary inflammatory and fibrosis. TGF-β1 plays an important role in profibrotic mediators through TGF-β receptors to activate the classical TGF-β/Smad signaling pathway (Fernandez and Eickelberg, 2012). In this study, we found that dihydromyricetin inhibited TGF-β1-induced fibroblast activation and ECM production via suppressing the TGF-β/Smad signaling pathway *in vitro* and also inhibited the migration of fibroblasts induced by TGF-β1.

5. Conclusions

In summary, we found dihydromyricetin is a potent SARS-CoV-2 M^{pro} inhibitor with potent enzymatic inhibition. It is also a potent effective inhibitor of pulmonary inflammatory and fibrosis, which is the respiratory complications of COVID-19. Dihydromyricetin maybe a hopeful therapeutic drug for antiviral and complications of COVID-19.

Consent for publication

Not applicable.

Availability of data and material

Data available on request from the authors.

Author contributions

Conception and design: HonggZ, CY, DongmL, and TX. Collection and assembly of data: XiaohL, YulW, MengqC and HaoR. Data analysis and interpretation: LZ, JialB, ShanfR, and DandG. Manuscript writing: MW and RonghS. Manuscript revision: MingjL and JianpL. All authors read and approved the final manuscript. All data were generated in-house, and no paper mill was used. All authors agree to be

accountable for all aspects of work ensuring integrity and accuracy.

Declaration of Competing Interests

The authors declare that they have no competing interests.

Funding

This study was supported by The National Natural Science Foundation of China [Grant 82070060], The Fundamental Research Funds for the Central University [Grant 735-63201241] and [Grant 735-63201239].

References

Abian, O., Ortega-Alarcon, D., Jimenez-Alesanco, A., Ceballos-Laita, L., Vega, S., Reyburn, H.T., Rizzuti, B., Velazquez-Campoy, A., 2020. Structural stability of SARS-CoV-2 3CLpro and identification of quercetin as an inhibitor by experimental screening. Int. J. Biol. Macromol. 164, 1693–1703.

Aleem, A., Kothadia, J.P., 2020. Remdesivir,statpearls, Treasure Island (FL).

Batool, F., Mughal, E.U., Zia, K., Sadiq, A., Naeem, N., Javid, A., Ul-Haq, Z., Saeed, M., 2020. Synthetic flavonoids as potential antiviral agents against SARS-CoV-2 main protease. J. Biomol. Struct. Dyn. 1–12.

Bhachoo, J., Beuming, T., 2017. Investigating protein-peptide interactions using the schrodinger computational suite. Methods Mol. Biol. 1561, 235–254.

Conti, P., Gallenga, C.E., Tete, G., Caraffa, A., Ronconi, G., Younes, A., Toniato, E., Ross, R., Kritas, S.K., 2020a. How to reduce the likelihood of coronavirus-19 (CoV-19 or SARS-CoV-2) infection and lung inflammation mediated by IL-1. J. Biol. Regul. Homeost. Agents 34, 333–338.

Conti, P., Ronconi, G., Caraffa, A., Gallenga, C.E., Ross, R., Frydas, I., Kritas, S.K., 2020b. Induction of pro-inflammatory cytokines (IL-1 and IL-6) and lung inflammation by Coronavirus-19 (COVI-19 or SARS-CoV-2): anti-inflammatory strategies. J. Biol. Regul. Homeost. Agents 34, 327–331.

Coronaviridae Study Group of the International Committee on Taxonomy of, V, 2020. The species severe acute respiratory syndrome-related coronavirus: classifying 2019-nCoV and naming it SARS-CoV-2. Nat. Microbiol. 5, 536–544.

Costanzo, M., De Giglio, M.A.R., Roviello, G.N., 2020. SARS-CoV-2: recent reports on antiviral therapies based on lopinavir/ritonavir, darunavir/umifenovir, hydroxychloroquine, remdesivir, favipiravir and other drugs for the treatment of the new coronavirus. Curr. Med. Chem. 27, 4536–4541.

Das, P., Majumder, R., Mandal, M., Basak, P., 2020. In-Silico approach for identification of effective and stable inhibitors for COVID-19 main protease (M(pro)) from flavonoid based phytochemical constituents of Calendula officinalis. J. Biomol. Struct. Dyn. 1–16.

Fernandez, I.E., Eickelberg, O., 2012. The impact of TGF-beta on lung fibrosis: from targeting to biomarkers. Proc. Am. Thorac. Soc. 9, 111–116.

Ghosh, R., Chakraborty, A., Biswas, A., Chowdhuri, S., 2020. Evaluation of green tea polyphenols as novel corona virus (SARS CoV-2) main protease (Mpro) inhibitors - an in silico docking and molecular dynamics simulation study. J. Biomol. Struct. Dyn. 1–13.

Gupta, S.P., 2020. Progress instudies on structural and remedial aspects of newly born coronavirus, SARS-CoV-2. Curr. Top. Med. Chem. 20, 2362–2378.

Ibrahim, M.A.A., Abdeljawaad, K.A.A., Abdelrahman, A.H.M., Hegazy, M.F., 2020. Natural-like products as potential SARS-CoV-2 M(pro) inhibitors: in-silico drug discovery. J. Biomol. Struct. Dyn. 1–13.

Ibrahim, M.A.A., Mohamed, E.A.R., Abdelrahman, A.H.M., Allemailem, K.S., Moustafa, M.F., Shawky, A.M., Mahzari, A., Hakami, A.R., Abdeljawaad, K.A.A., Atia, M.A.M., 2021. Rutin and flavone analogs as prospective SARS-CoV-2 main protease inhibitors: In silico drug discovery study. J. Mol. Graph. Model. 105, 107904.

Jiang, D., Liang, J., Hodge, J., Lu, B., Zhu, Z., Yu, S., Fan, J., Gao, Y., Yin, Z., Homer, R., Gerard, C., Noble, P.W., 2004. Regulation of pulmonary fibrosis by chemokine receptor CXCR3. J. Clin. Invest. 114, 291–299.

Jin, Z., Du, X., Xu, Y., Deng, Y., Liu, M., Zhao, Y., Zhang, B., Li, X., Zhang, L., Peng, C., Duan, Y., Yu, J., Wang, L., Yang, K., Liu, F., Jiang, R., Yang, X., You, T., Liu, X., Yang, X., Bai, F., Liu, H., Liu, X., Guddat, L.W., Xu, W., Xiao, G., Qin, C., Shi, Z., Jiang, H., Rao, Z., Yang, H., 2020. Structure of M(pro) from SARS-CoV-2 and discovery of its inhibitors. Nature 582, 289–293.

Lamb, Y.N., 2020. Remdesivir: First approval. Drugs 80, 1355–1363.

Li, X., Bi, Z., Liu, S., Gao, S., Cui, Y., Huang, K., Huang, M., Mao, J., Li, L., Gao, J., Sun, T., Zhou, H., Yang, C., 2019. Antifibrotic mechanism of cinobufagin in bleomycin-induced pulmonary fibrosis in mice. Front. Pharmacol. 10, 1021.

Li, X., Yu, H., Liang, L., Bi, Z., Wang, Y., Gao, S., Wang, M., Li, H., Miao, Y., Deng, R., Ma, L., Luan, J., Li, S., Liu, M., Lin, J., Zhou, H., Yang, C., 2020. Myricetin ameliorates bleomycin-induced pulmonary fibrosis in mice by inhibiting TGF-beta signaling via targeting HSP90beta. Biochem. Pharmacol. 178, 114097.

Luo, H., Tang, Q.L., Shang, Y.X., Liang, S.B., Yang, M., Robinson, N., Liu, J.P., 2020. Can Chinese medicine be used for prevention of corona virus disease 2019 (COVID-19)? A review of historical classics, research evidence and current prevention programs. Chin. J. Integr. Med. 26, 243–250.

Moirangthem, D.S., Surbala, L., 2020. Remdesivir (GS-5734) in COVID-19 therapy: The fourth chance. Curr. Drug Targets.

Morse, J.S., Lalonde, T., Xu, S., Liu, W.R., 2020. Learning from the past: Possible urgent prevention and treatment options for severe acute respiratory infections caused by 2019-nCoV. ChemBioChem 21, 730–738.

Muramatsu, T., Kim, Y.T., Nishii, W., Terada, T., Shirouzu, M., Yokoyama, S., 2013. Autoprocessing mechanism of severe acute respiratory syndrome coronavirus 3C-like protease (SARS-CoV 3CLpro) from its polyproteins. FEBS J. 280, 2002–2013.

Nguyen, T.T., Woo, H.J., Kang, H.K., Nguyen, V.D., Kim, Y.M., Kim, D.W., Ahn, S.A., Xia, Y., Kim, D., 2012. Flavonoid-mediated inhibition of SARS coronavirus 3C-like protease expressed in Pichia pastoris. Biotechnol. Lett. 34, 831–838.

Ning, W., Li, C.J., Kaminski, N., Feghali-Bostwick, C.A., Alber, S.M., Di, Y.P., Otterbein, S.L., Song, R., Hayashi, S., Zhou, Z., Pinsky, D.J., Watkins, S.C., Pilewski, J.M., Sciurba, F.C., Peters, D.G., Hogg, J.C., Choi, A.M., 2004. Comprehensive gene expression profiles reveal pathways related to the pathogenesis of chronic obstructive pulmonary disease. Proc. Natl. Acad. Sci. U. S. A. 101, 14895–14900.

Ozma, M.A., Maroufi, P., Khodadadi, E., Kose, S., Esposito, I., Ganbarov, K., Dao, S., Esposito, S., Dal, T., Zeinalzadeh, E., Kafil, H.S., 2020. Clinical manifestation, diagnosis, prevention and control of SARS-CoV-2 (COVID-19) during the outbreak period. Infez. Med. 28, 153–165.

Sanders, J.M., Monogue, M.L., Jodlowski, T.Z., Cutrell, J.B., 2020. Pharmacologic treatments for coronavirus disease 2019 (COVID-19): A review. JAMA 323, 1824–1836.

Solnier, J., Fladerer, J.P., 2020. Flavonoids: A complementary approach to conventional therapy of COVID-19? Phytochem. Rev. 1–23.

Vijayakumar, B.G., Ramesh, D., Joji, A., Jayachandra Prakasan, J., Kannan, T., 2020. In silico pharmacokinetic and molecular docking studies of natural flavonoids and synthetic indole chalcones against essential proteins of SARS-CoV-2. Eur. J. Pharmacol. 886, 173448.

Vora, A., Tiwaskar, M., 2020. Favipiravir. J. Assoc. Physicians India 68, 91–92.

Wang, C., Horby, P.W., Hayden, F.G., Gao, G.F., 2020. A novel coronavirus outbreak of global health concern. Lancet 395, 470–473.

Wu, A., Peng, Y., Huang, B., Ding, X., Wang, X., Niu, P., Meng, J., Zhu, Z., Zhang, Z., Wang, J., Sheng, J., Quan, L., Xia, Z., Tan, W., Cheng, G., Jiang, T., 2020. Genome composition and divergence of the novel coronavirus (2019-nCoV) originating in China. Cell Host Microbe. 27, 325–328.

Wu, A., Wang, Y., Zeng, C., Huang, X., Xu, S., Su, C., Wang, M., Chen, Y., Guo, D., 2015. Prediction and biochemical analysis of putative cleavage sites of the 3C-like protease of Middle East respiratory syndrome coronavirus. Virus Res. 208, 56–65.

Wu, S., Liu, B., Zhang, Q., Liu, J., Zhou, W., Wang, C., Li, M., Bao, S., Zhu, R., 2013. Dihydromyricetin reduced Bcl-2 expression via p53 in human hepatoma HepG2 cells. PLoS One 8, e76886.

Zhang, J., Chen, Y., Luo, H., Sun, L., Xu, M., Yu, J., Zhou, Q., Meng, G., Yang, S., 2018. Recent update on the pharmacological effects and mechanisms of dihydromyricetin. Front. Pharmacol. 9, 1204.

Zhu, N., Zhang, D., Wang, W., Li, X., Yang, B., Song, J., Zhao, X., Huang, B., Shi, W., Lu, R., Niu, P., Zhan, F., Ma, X., Wang, D., Xu, W., Wu, G., Gao, G.F., Tan, W., China Novel Coronavirus, I., Research, T., 2020. A novel coronavirus from patients with pneumonia in China, 2019. N. Engl. J. Med. 382, 727–733.